Electronic Supplementary Material (ESI) for Materials Advances.

Supplementary Information

Asymmetric-Donors(D_2D_2')-Acceptor(A) Conjugates for Accessing Simultaneous Intrinsic Blue-RTP and Blue-TADF

*Harsh Bhatia, Debdas Ray**

Advanced Photofunctional Materials Laboratory, Department of Chemistry, Shiv Nadar University, NH-91, Tehsil Dadri, District Gautam Buddha Nagar, Uttar Pradesh, 201314, India.

Corresponding Author: debdas.ray@snu.edu.in

Table of contents

1. Experimental details

General. All the reagents and deuterated solvents were obtained from commercial sources and used without any further purification, unless otherwise mentioned. Dimethyl formamide (DMF) was dried and distilled over calcium hydride. ^{1}H and ^{13}C NMR spectra were recorded in Bruker AVHDN 400 with working frequencies of 400.245 MHz for ^{1}H and 100.6419 MHz for ^{13}C nuclei, respectively, using $CDCl_3$. Chemical shifts were quoted in ppm relative to tetramethylsilane, using residual solvent peak as a reference standard. Steady state absorbance

was measured using Cary 8454 (Agilent Technologies) spectrophotometer. Steady-state emission, phosphorescence, and lifetime analysis of both fluorescence and phosphorescence were recorded by Fluorolog-3 spectrofluorometer (HORIBA; Model, FL3-2-IHR320).[1] The phosphorescence spectra were recorded by Flash-lamp using detector delay of 50 μs and keeping the sample window 3 times the lifetime of the phosphor. Absolute photoluminescence quantum yield measurements of the compounds in films were recorded on Edinburgh FS5 spectrofluorometer by using an integrating sphere (SC-30). Temperature-dependent measurements were performed using liquid N_2 Dewar assembly attached with HORIBA Fluorolog-3 spectrofluorometer. All the fluorescence lifetime measurements and the time resolved emission spectra (TRES) were measured with the nano-LED (λ_{ex} = 370 nm) using the data station software. All the phosphorescent lifetime and delay-dependent TRES measurements were performed with gated detector using the spectra-LED (λ_{ex} = 370 nm) with Data Station software (Fluorolog-3 spectrofluorometer).

2. Synthesis of CPPN, CPPNF, PPN and PPNF

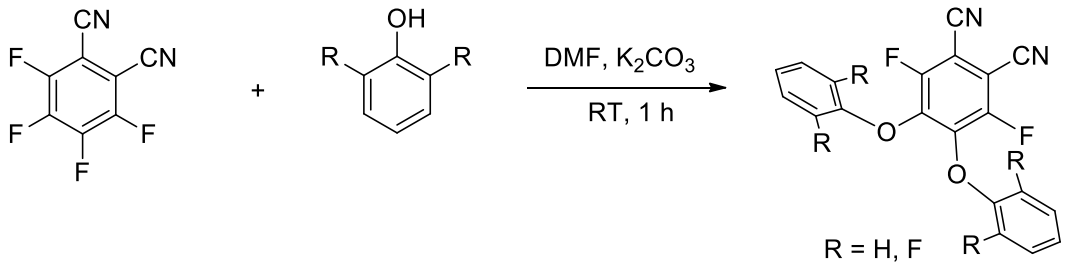

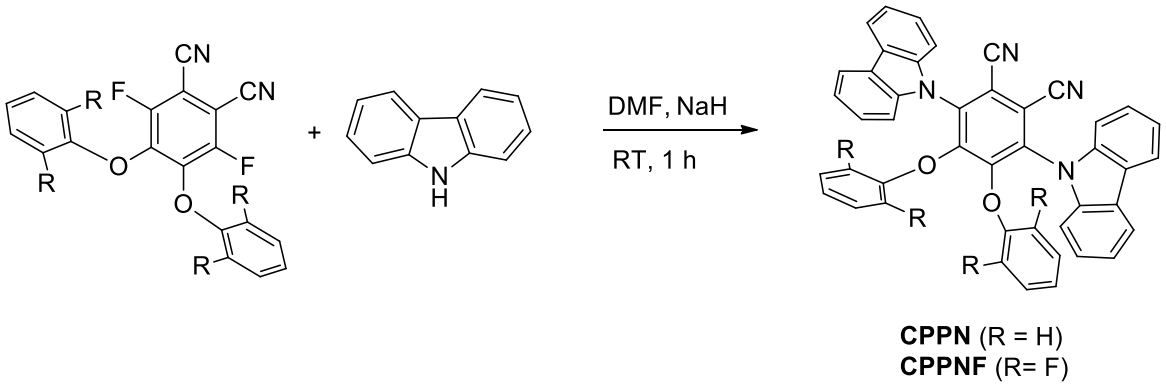

Scheme S1. The general synthesis scheme of **CPPN** and **CPPNF**.

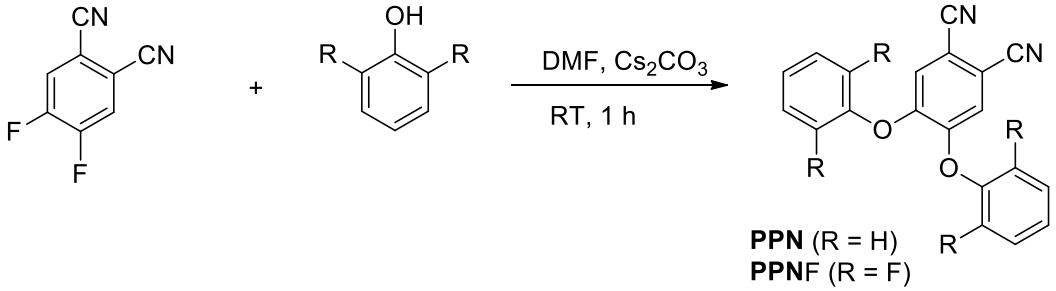

Scheme S2. The general synthesis scheme of **PPN** and **PPNF**.

Synthesis of CPPN and CPPNF: Anhydrous K_2CO_3 (3.0 equiv.) was added to dry DMF in 25 mL two-neck round bottom flask under nitrogen atmosphere. Then, phenol or 2-fluorophenol, (2.2 equiv.) was added immediately to the reaction mixture at room-temperature. After 5 minutes, tetrafluorophathonitrile (1.0 equiv.) was added at a time under constant stirring. After 1 hour, TLC was checked and reaction was stopped. The reaction mixture was poured into ice-cold water. The precipitate was washed with 1M NaOH solution and extracted with dichloromethane. This organic layer was dried with Na_2SO_4 and purified with column chromatography (SiO_2: Ethyl acetate: Hexane, 5:95) to afford the intermediate compound. For the second step, sodium hydride (NaH) (2.5 equiv.) was added to dry DMF in 25 mL 2-neck round bottom flask under nitrogen atmosphere. After 5 minutes, carbazole was added to this reaction mixture. When the evolution of the hydrogen gas was stopped, intermediate obtained in the earlier reaction step was added. The reaction was allowed to proceed till the starting material (intermediate) was consumed. The progress of the reaction

was confirmed by TLC. The reaction mixture was poured into ice cold water and extracted with dichloromethane. This organic layer was dried with Na_2SO_4 and purified with column chromatography (SiO_2: Ethyl acetate: Hexane, 5:95) to afford the purified product (yield, ~50%)

Synthesis of PPN and PPNF: Cs_2CO_3 (3.0 equiv.) was added to dry DMF in 25 mL two-neck round bottom flask under nitrogen atmosphere. Immediately, phenol or 2-fluorophenol, (2.2 equiv.) was added to the reaction mixture at room temperature, and after 5 minutes 4,5-difluorophtalonitrile (1.0 equiv.) was added under constant stirring. The reaction was stopped after 1 hour. The reaction mixture was poured into cold water and extracted with dichloromethane. The organic layer was dried with Na_2SO_4 and purified with column chromatography (SiO_2: Ethyl acetate: Hexane, 2:98) to afford the purified product (yield, 90%).

3. ^{1}H and ^{13}C NMR spectra of CPPN, CPPNF, PPN and PPNF.

(3r,6r)-3,6-di(9H-carbazol-9-yl)-4,5-diphenoxyphthalonitrile (CPPN), ^{1}H NMR ($CDCl_3$): δ 7.95 (d, J = 7.72 Hz, 2H), 7.48 (t, J = 8.12 Hz, 2H), 7.30 (t, J = 7.56 Hz, 2H), 7.25 (d, 2H), 6.67 (t, J = 8.04 Hz, 2H), 6.57 (t, J = 7.4 Hz, 1H), 6.18 (d, J = 8.24 Hz, 2H). **^{13}C NMR ($CDCl_3$):** 155.31, 151.85, 139.11, 135.08, 128.76, 126.22, 124.24, 123.84, 121.61, 120.6, 115.52, 114.81, 112.26, 109.97.

(3r,6r)-3,6-di(9H-carbazol-9-yl)-4,5-bis(2,6-difluorophenoxy)phthalonitrile (CPPNF), ^{1}H NMR ($CDCl_3$): δ 7.96 (d, J = 7.68 Hz, 2H), 7.48 (t, J = 8.12 Hz, 2H), 7.32 (t, J = 7.64 Hz, 2H), 7.27 (d, 2H), 6.47 (m, 1H), 6.28 (t, J = 8.52 Hz, 2H). **^{13}C NMR ($CDCl_3$):** 139.26, 132.88, 126.54, 124.06, 121.72, 120.40, 114.83, 111.88, 111.63, 111.47, 109.80.

4,5-diphenoxyphthalonitrile (PPN), ^{1}H NMR ($CDCl_3$): δ 7.46 (t, J = 8.44 Hz, 2H), 7.29 (t, J = 7.44 Hz, 1H), 7.16 (s, 1H), 7.08 (d, J = 9.56 Hz, 2H). **^{13}C NMR ($CDCl_3$):** 154.14, 151.97, 130.58, 125.97, 122.01, 119.9, 115.00, 110.4.

4,5-bis(2,6-difluorophenoxy)phthalonitrile (PPNF), ^{1}H NMR ($CDCl_3$): δ 7.30 (m, 1H), 7.10 (t, J = 8.84 Hz, 2H). **^{13}C NMR ($CDCl_3$):** 156.54, 154.03, 150.14, 127.20, 127.11, 127.01, 119.90, 114.67, 113.20, 113.16, 112.99, 111.20.

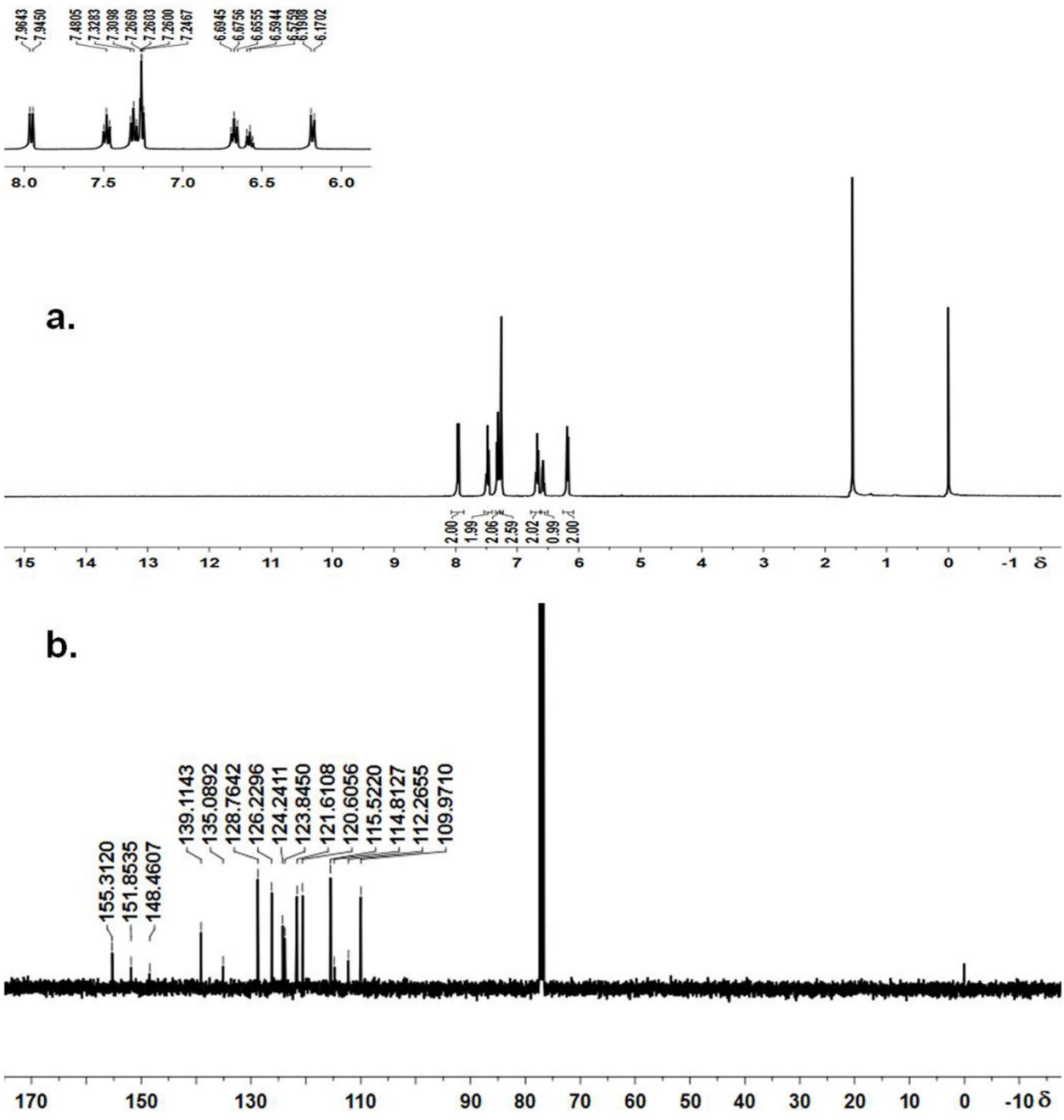

Figure S1. The (a) ^{1}H NMR and (b) ^{13}C NMR spectra of **CPPN**.

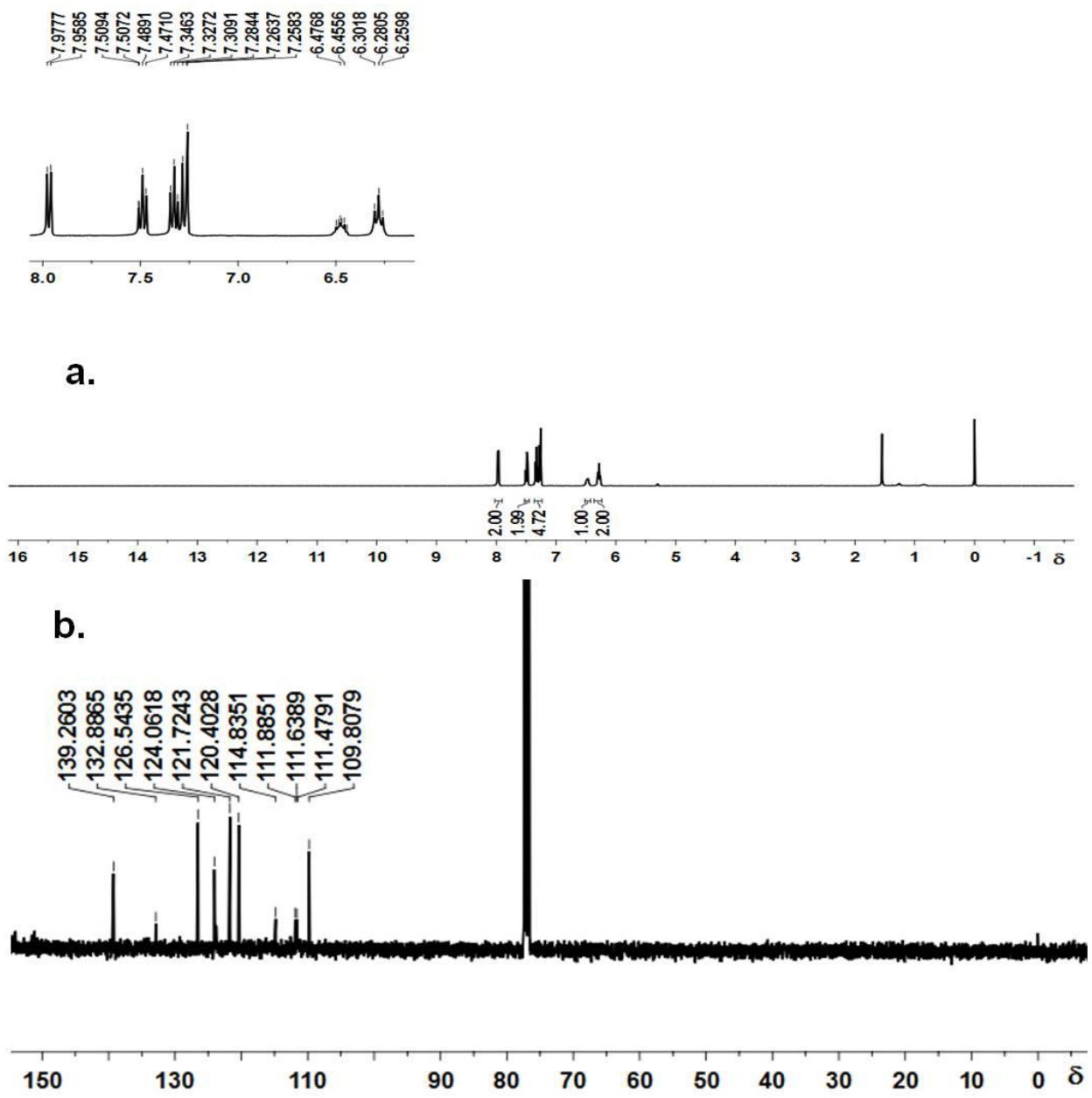

Figure S2. The (a) ^{1}H NMR and (b) ^{13}C NMR spectra of **CPPNF**.

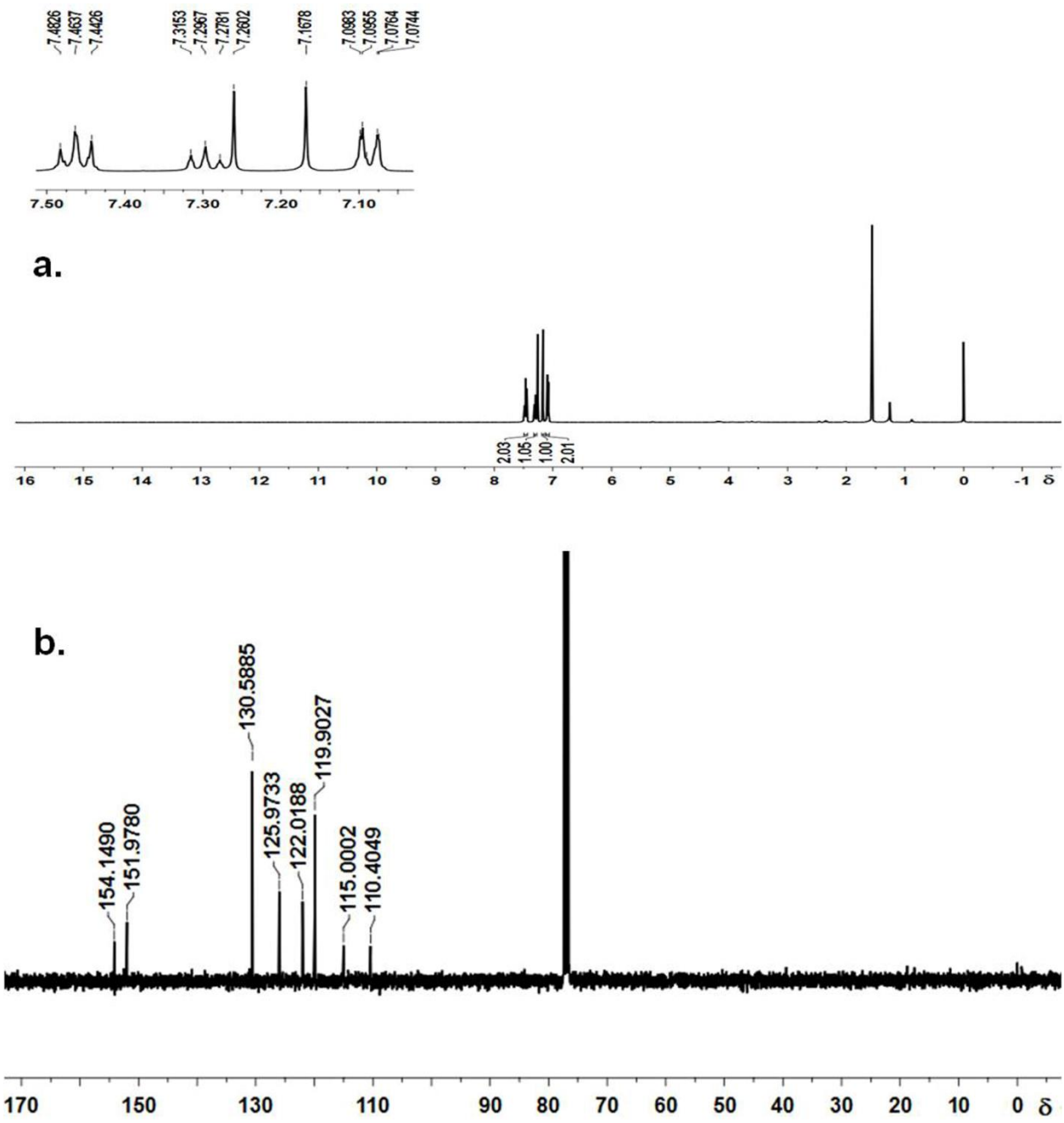

Figure S3. The (a) ^{1}H NMR and (b) ^{13}C NMR spectra of **PPN**.

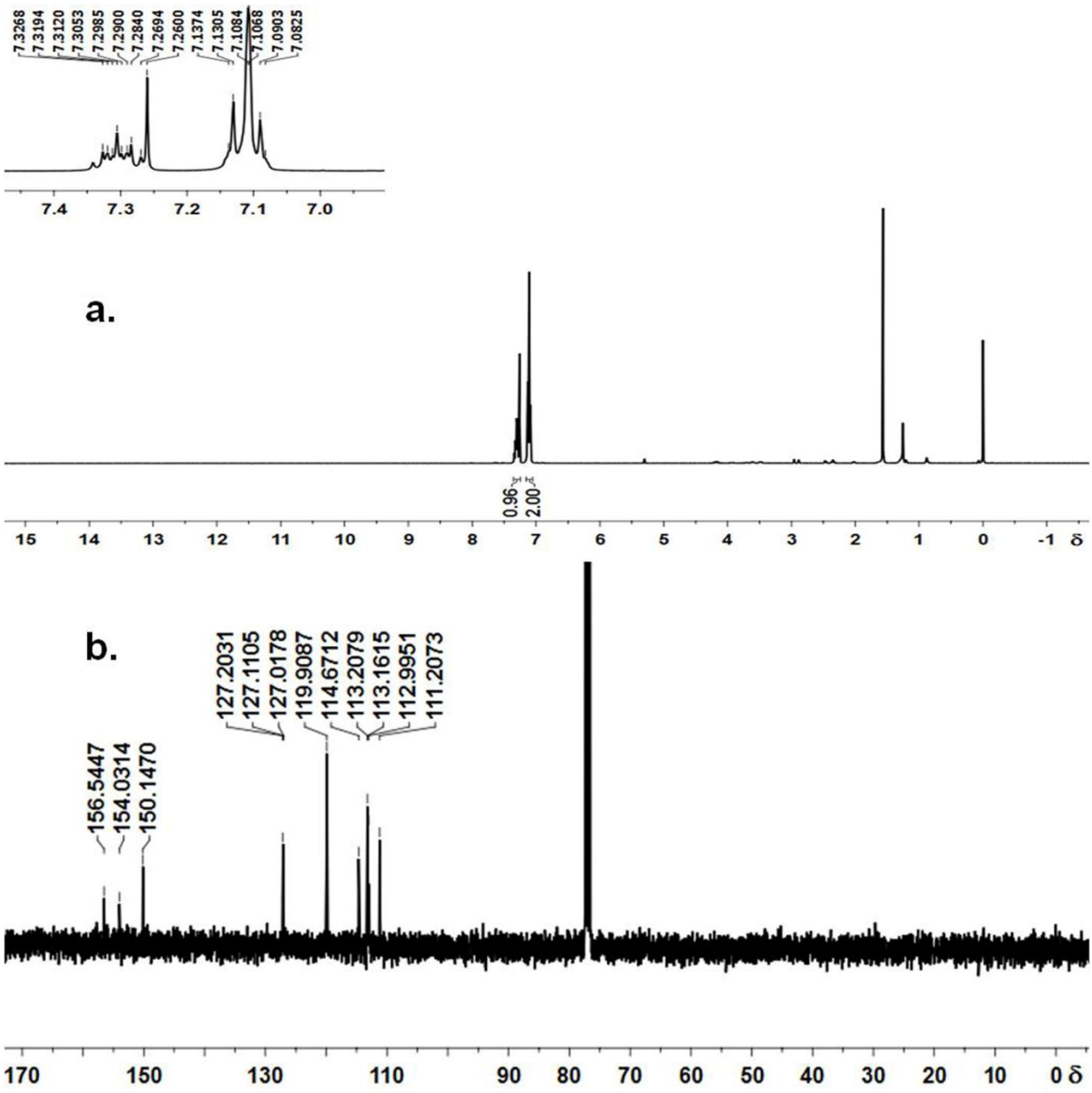

Figure S4. The (a) ^{1}H NMR and (b) ^{13}C NMR spectra of **PPNF.**

4. Photophysical studies in solutions

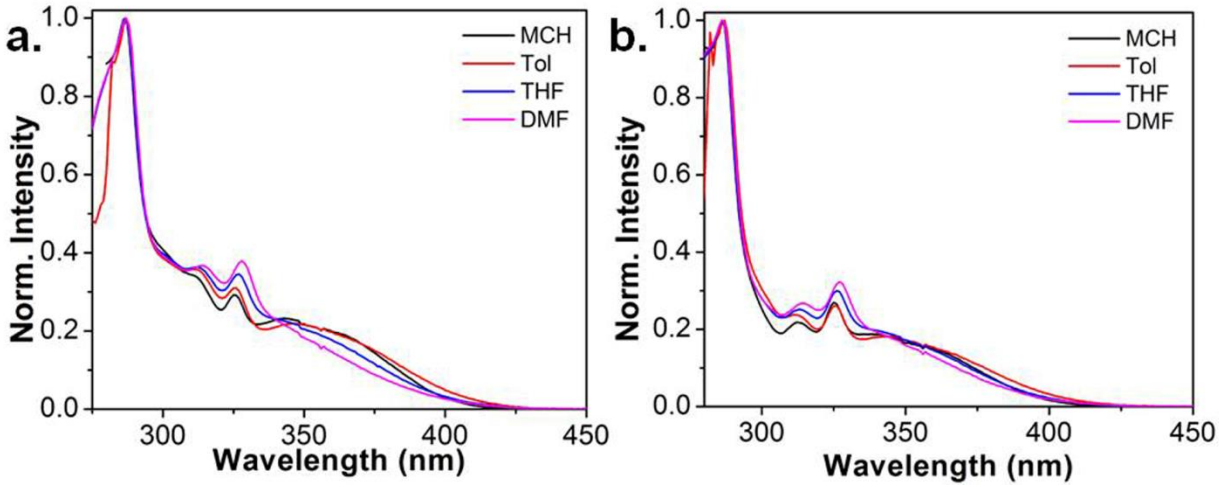

Figure S5. UV-visible spectra of (a) **CPPN** and (b) **CPPNF** in range of solvents under ambient conditions (concentration = 1×10^{-5} M).

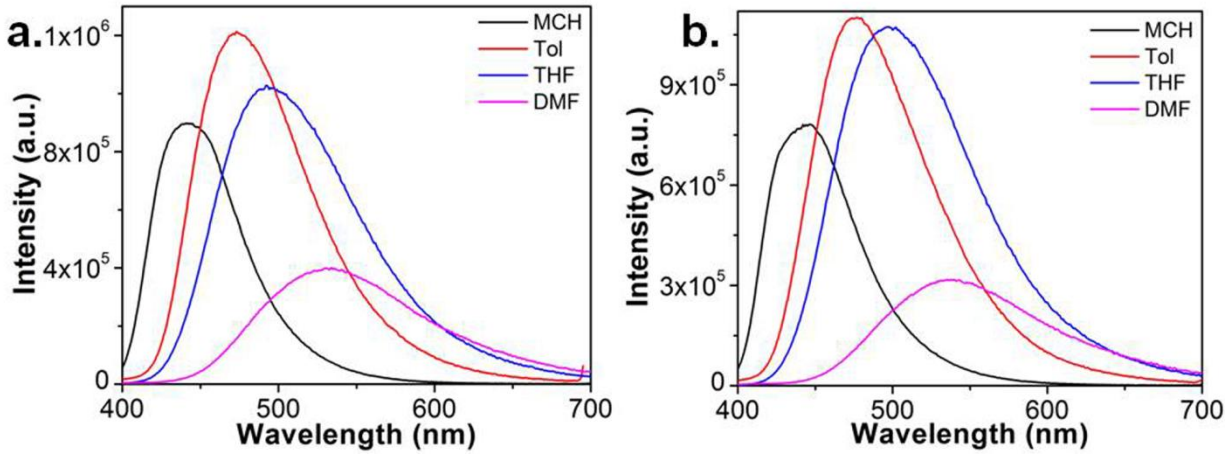

Figure S6. Solvent-dependent steady state emission spectra of (a) **CPPN** and (b) **CPPNF** under ambient conditions (λ_{ex} = 350 nm, concentration = 1×10^{-5} M).

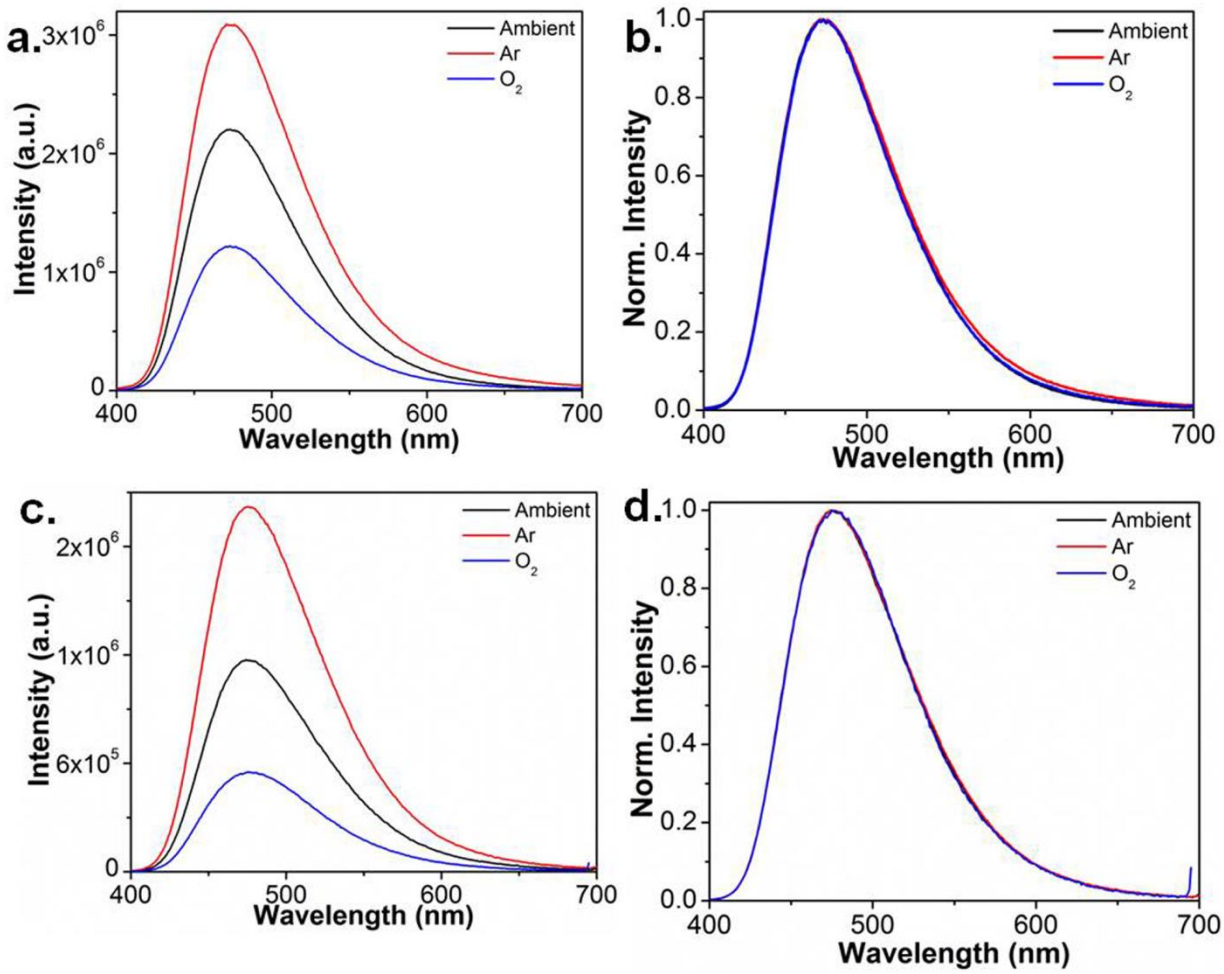

Figure S7. Steady state emission spectra of (a, b) **CPPN**, and (c, d) **CPPNF** in toluene under ambient, deoxygenated and oxygenated conditions (λ_{ex} = 350 nm, concentration = 1×10^{-5} M).

5. Photophysical studies in Films.

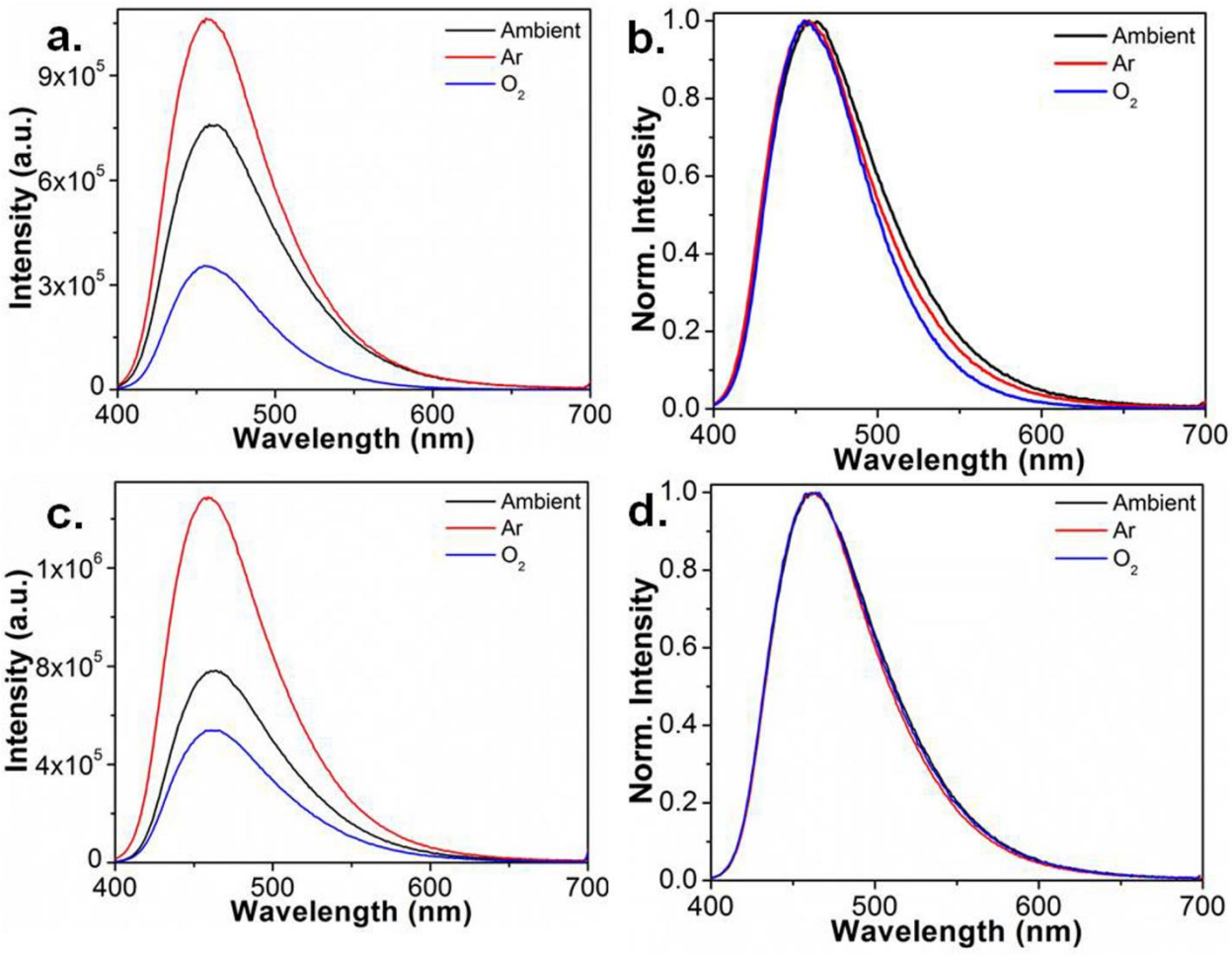

Figure S8. Steady state emission spectra of (a, b) **CPPN**, and (c, d) **CPPNF** in 0.1% PMMA films under ambient, deoxygenated and oxygenated conditions (λ_{ex} = 350 nm).

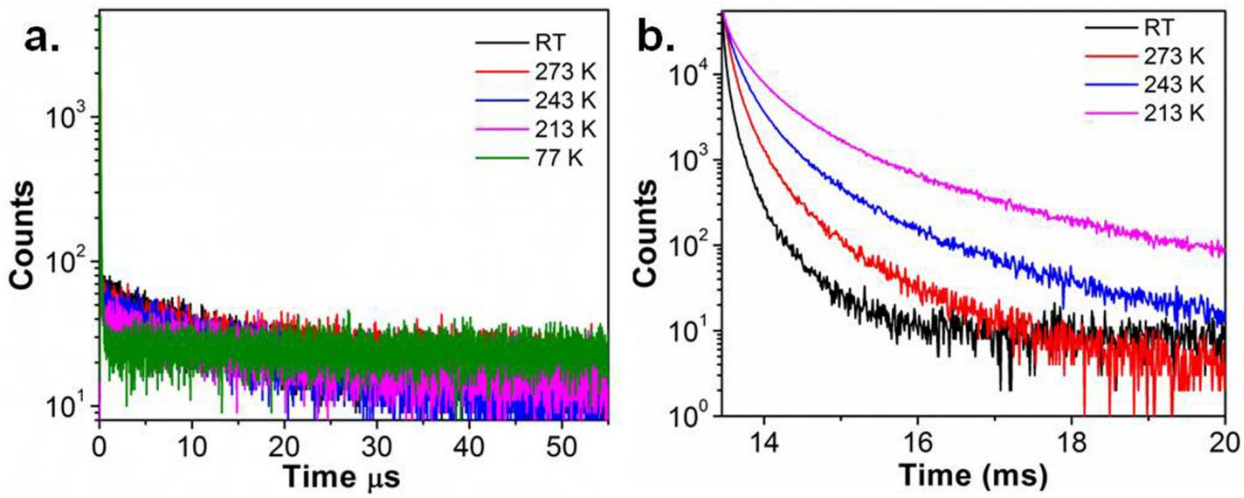

Figure S9. Temperature-dependent (a) fluorescence and (b) phosphorescence decay analysis of **CPPNF** 0.1% PMMA films (λ_{ex} = 370 nm).

Table S1: Temperature-dependent fluorescence lifetime measurements in PMMA.

	CPPN	**CPPNF**
Temperature	**τ**	**τ**
273 K	12.20 ns (49.59%), 9.96 μs (50.41%)	14.12 ns (40.26%), 10.63 μs (59.74%)
243 K	13.94 ns (55.27%), 9.38 μs (44.73%)	16.13 ns (34.09%), 12.61 μs (65.91%)
213 K	11.56 ns (85.5%), 4.19 μs (14.5%)	16.80 ns (59.27%), 7.41 μs (40.73%)
77 K	11.31 ns (79.56%), 63.1 ns (20.44%)	12.86 ns (70.56%), 68.25 ns (29.44%)

Table S2: Temperature-dependent phosphorescence lifetimes measurements in PMMA.

	CPPN	**CPPNF**
Temperature	**τ (ms)**	**τ (ms)**
RT	0.05 (25.98%), 0.17 (58.05%), 0.61 (15.97%)	0.14 (51.05%), 0.57 (12.12%), 0.04 (36.83%)
273 K	0.11 (44.17%), 0.35 (45.46%), 1.27 (10.37%)	0.26 (46.46%), 0.08 (43.65%), 1.05 (9.9%)
243 K	0.34 (46.49%), 1.03 (44.60%), 4.02 (8.91%)	0.45 (47.45%), 1.97 (10.45%), 0.13 (42.11%)
213 K	3.59 (40.52%), 1.16 (49.67%), 13.27 (9.81%)	1.35 (48.49%), 5.79 (12.19%), 0.38 (39.32%)

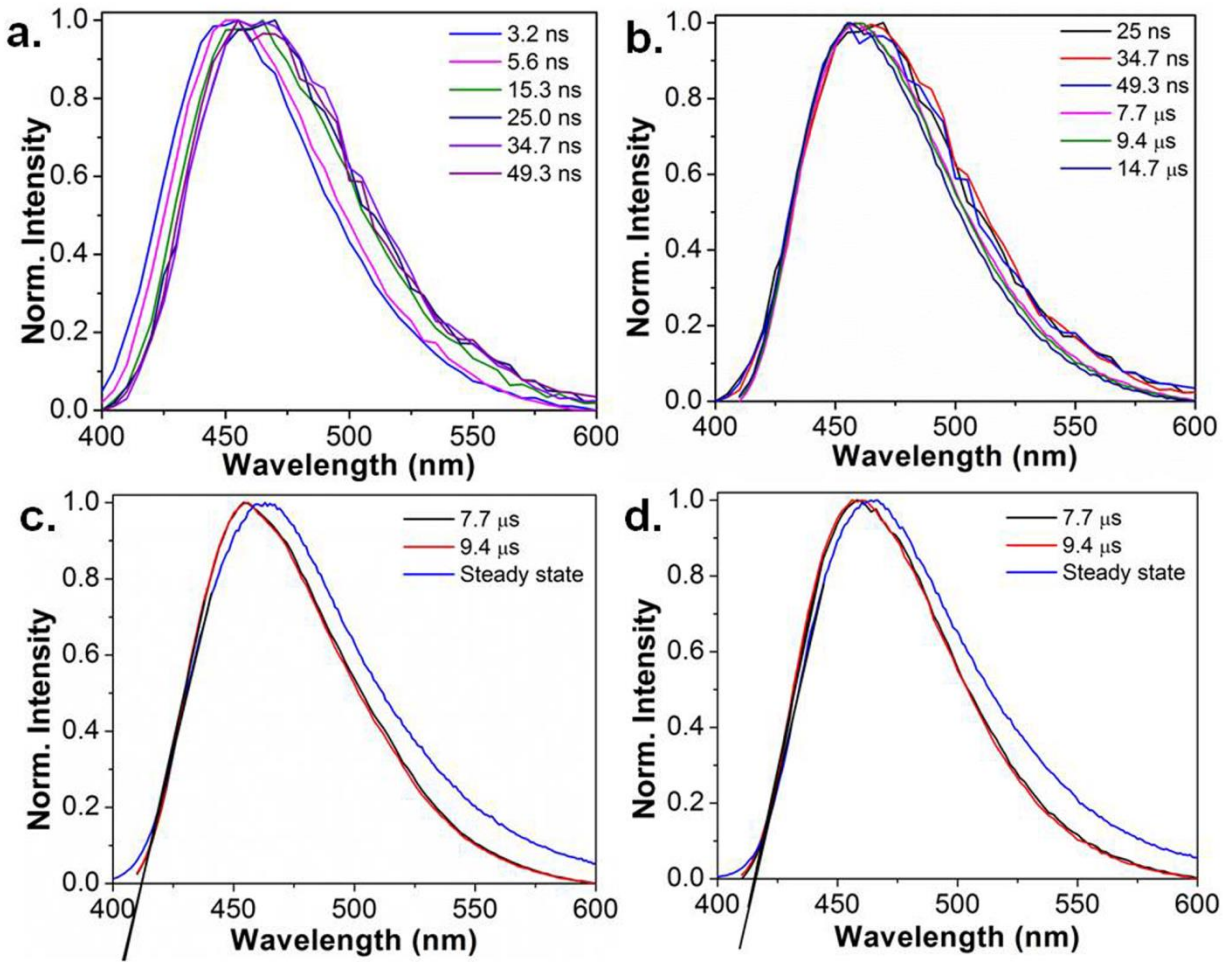

Figure S10. (a, b) Time resolved emission spectra (TRES) of **CPPNF** in 0.1% PMMA films and comparison of steady state and TRES data of (c) **CPPN** and (d) **CPPNF** at ambient conditions.

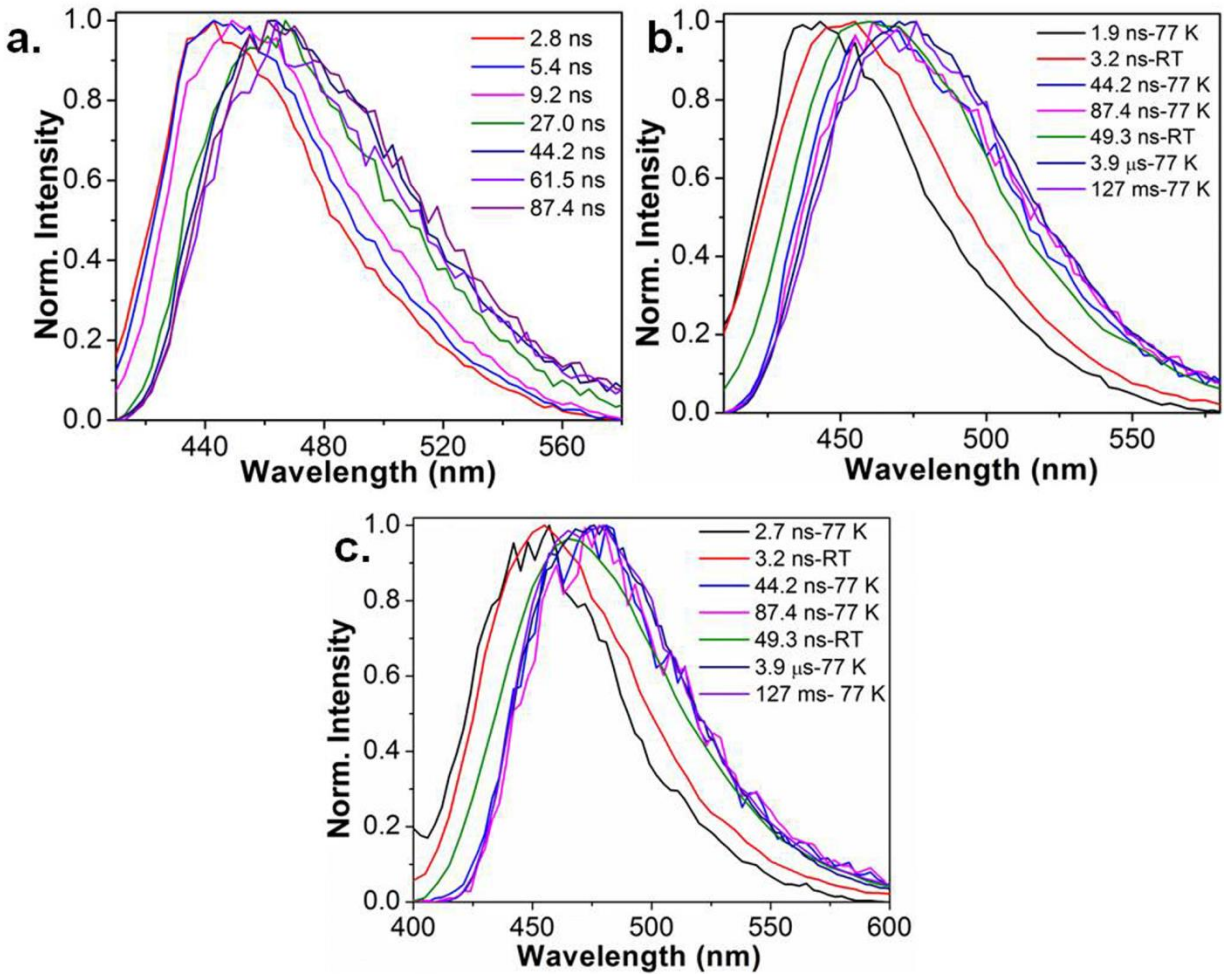

Figure S11. Time resolved emission spectra of PMMA films (a) at 77 K (**CPPNF**), (b) RT and 77 K (**CPPNF**) and (c) RT and 77 K (**CPPN**).

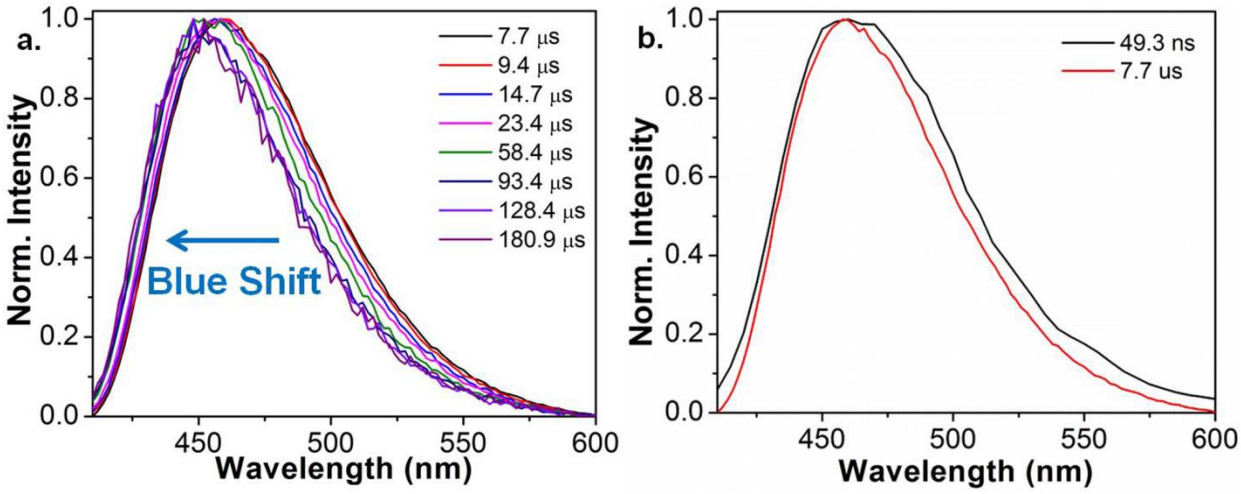

Figure S12. Time resolved emission spectra of PMMA films of **CPPNF** (a) with 6.8 μs detector delay (b) at different time scale at ambient conditions.

TRES data recorded with different delay times under different conditions showing change in the emission behavior (Figure S13). The spectra initially obtained at 7.7 μs blue shift to a higher energy state at 3.06 and 3.05 eV (180.9 μs) in the case of CPPN and CPPNF, respectively. While the spectra obtained at 127 ms recorded after the detector delay of 7 ms was found to be red shifted and highly stabilized as compared to the RTP band observed at 180.9 μs. The species obtained at 180.9 μs and 127 ms were characterized as $^{3}LE_{PPN}$ and $^{3}CT_{CzPN}$ .The spectra obtained at 180.9 μs and 127 ms is used to calculate the energy of the state triplet state while the spectra immediately obtained after 6.8 μs of delay is used to calculate the energy of the $^{1}CT_{CzPN}$ state.

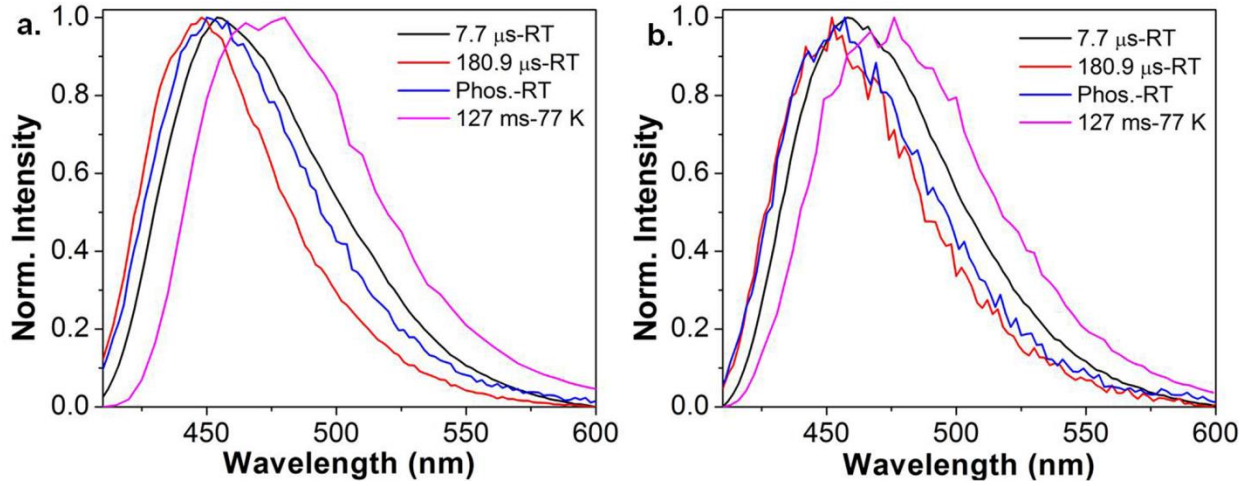

Figure S13. Phosphorescence emission and time resolved emission studies of (a) **CPPN** and (b) **CPPNF** with 6.8 μs and 7 ms of detector delay.

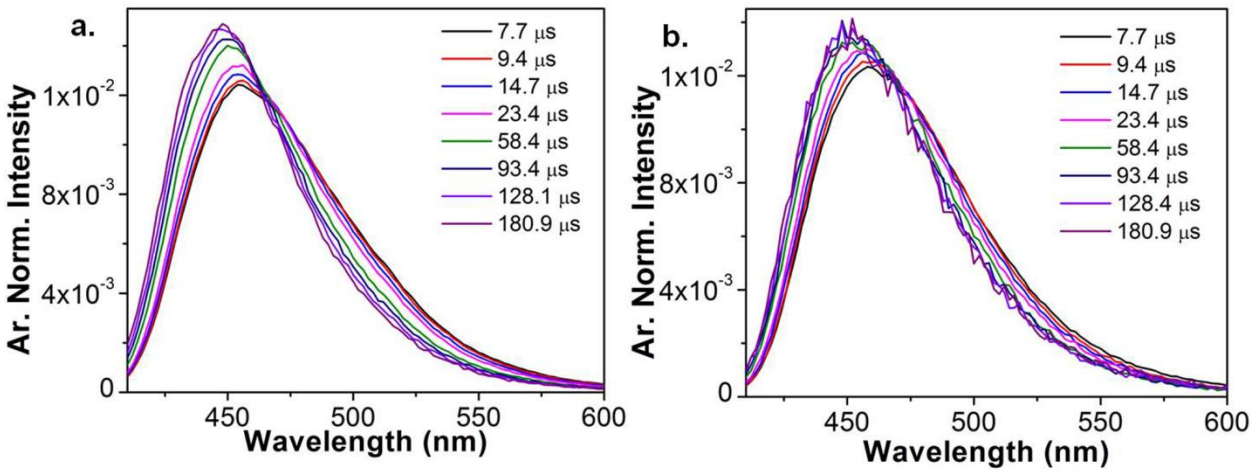

Figure S14. Time resolved area normalized emission spectra (TRANES) of (a) **CPPN** and (b) **CPPNF** when recorded after 6.8 μs of detector delay at RT.

TRES measurements of **CPPN** and **CPPNF** in PMMA matrix recorded at 77 K with delay of 3.4 μs and 110 ms have shown in Figure S15. No shift in the emission spectra was recorded which shows that only single excited state is responsible for the emission at 77 K. Moreover, the spectra remain unchanged with increasing the delay from 3.4 μs to 110 ms which further proves that emission occcurs from ^{3}CT state.

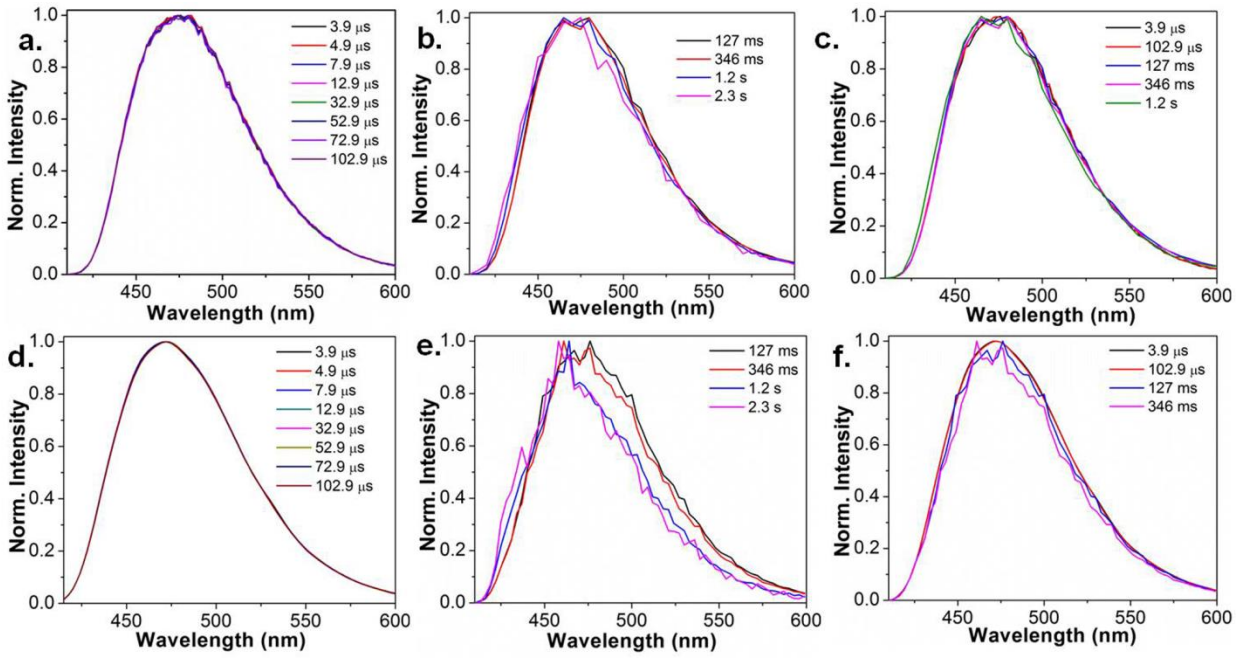

Figure S15. Time resolved emission spectra of (a-c) **CPPN** and (d-f) **CPPNF** at 77 K in PMMA films with detector delay of 3.4 μs and 110 ms.

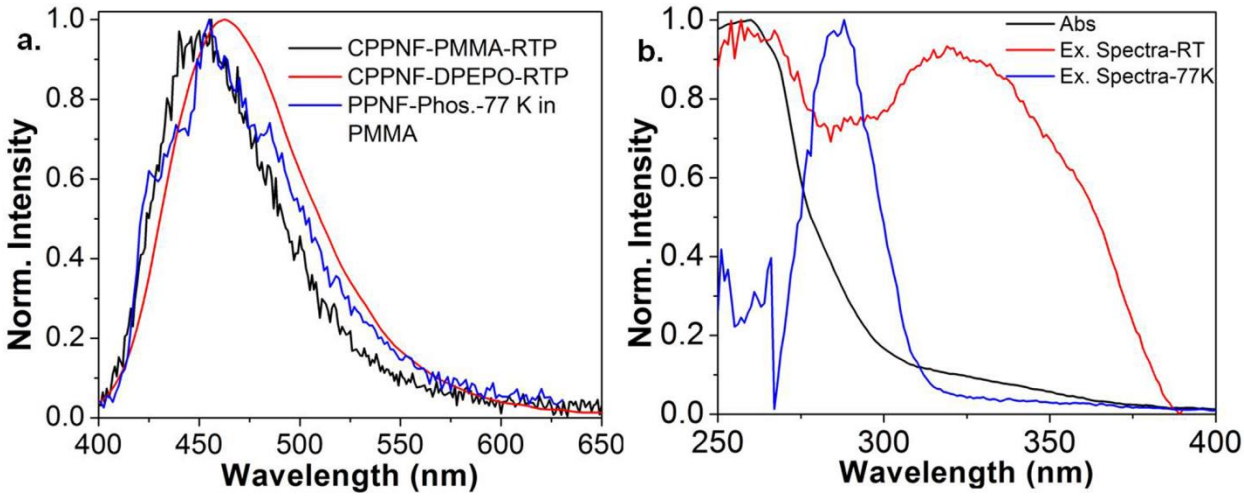

Figure S16. (a) Phosphorescence emission spectra of **CPPNF**, **PPNF** (b) Absorption and excitation spectra of **PPN** in PMMA.

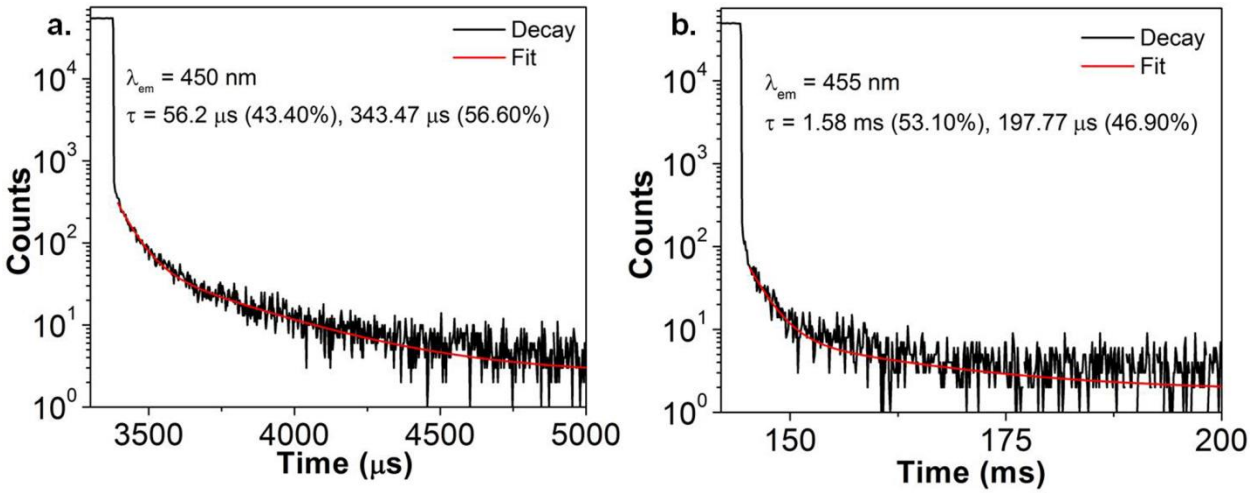

Figure S17. Phosphorescence lifetime of (a) **PPN** and (b) **PPNF** in 0.1% PMMA films (λ_{ex} = 370 nm).

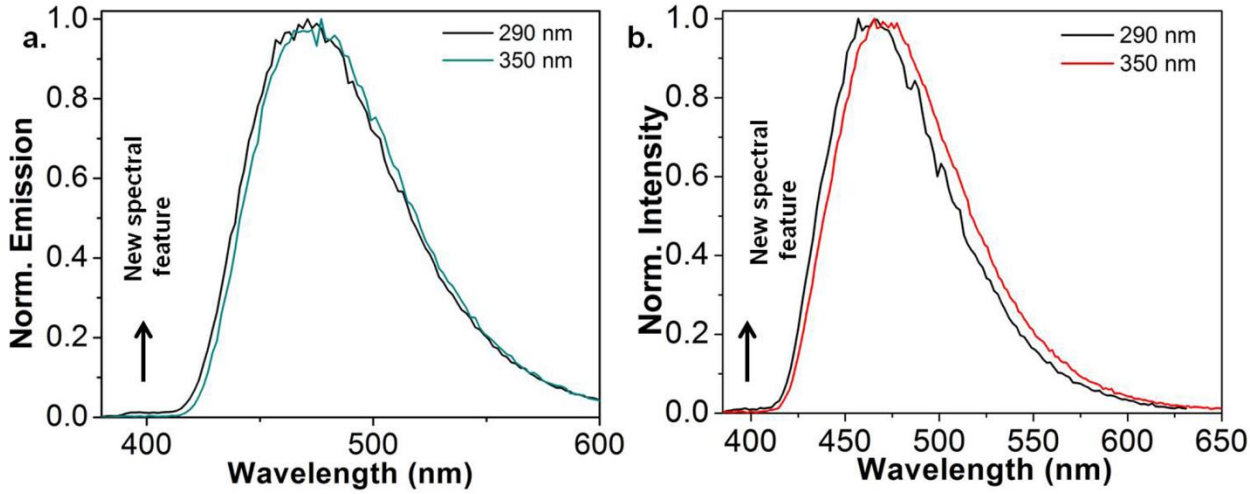

Figure S18. Phosphorescence emission at 77 K (a) **CPPN** and (b) **CPPNF** in PMMA.

The Figure S19 shows comparison of the steady state and phosphorescence emission spectra measured in PMMA and DPEPO (λ_{ex} = 350 nm). Broadening of the emission bands along with red shift of both emission spectra was observed while changing the host matrix from non-polar PMMA to polar DPEPO.

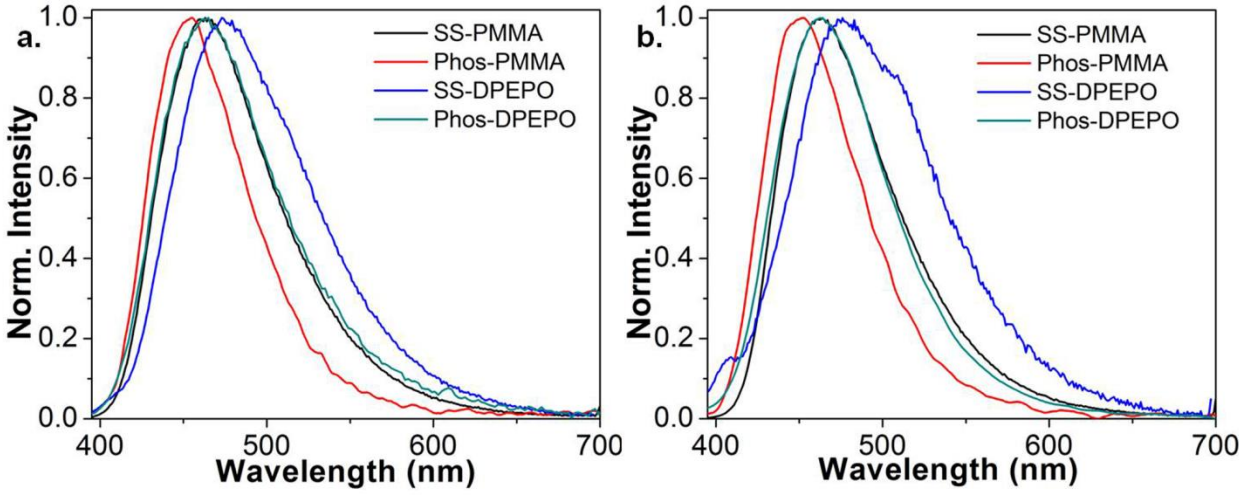

Figure S19. Steady state and phosphorescence emission of (a) **CPPN** and (b) **CPPNF** in 0.1% PMMA and DPEPO (λ_{ex} = 350 nm) at ambient conditions.

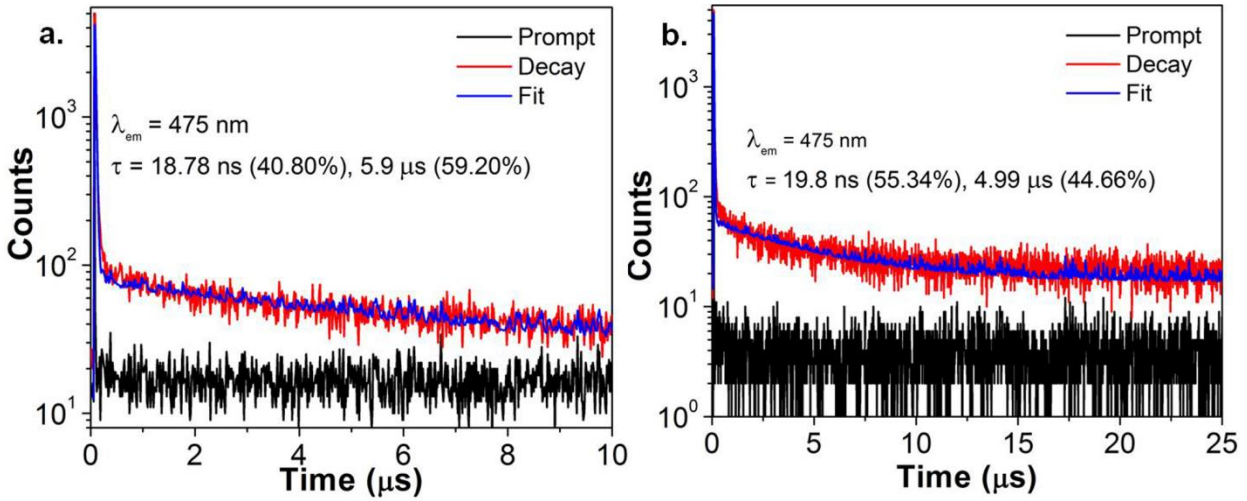

Figure S20. TCSPC analysis of 0.1% DPEPO films of (a) **CPPN** and (b) **CPPNF** (λ_{ex} = 370 nm) at ambient conditions.

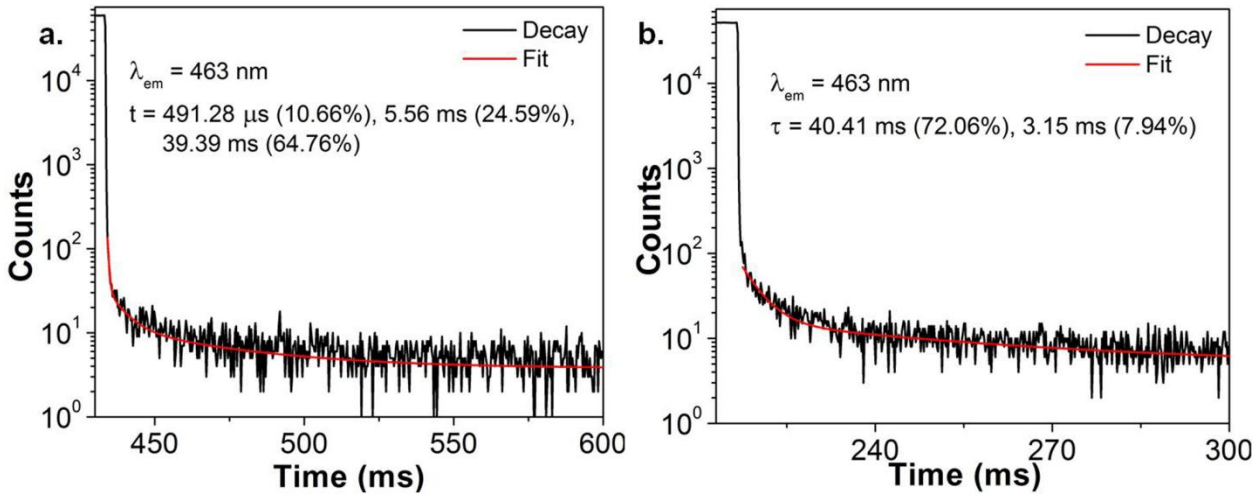

Figure S21. Phosphorescence lifetime measurements of (a) **CPPN** and (b) **CPPNF** in 0.1% DPEPO (λ_{ex} = 370 nm) at ambient conditions.

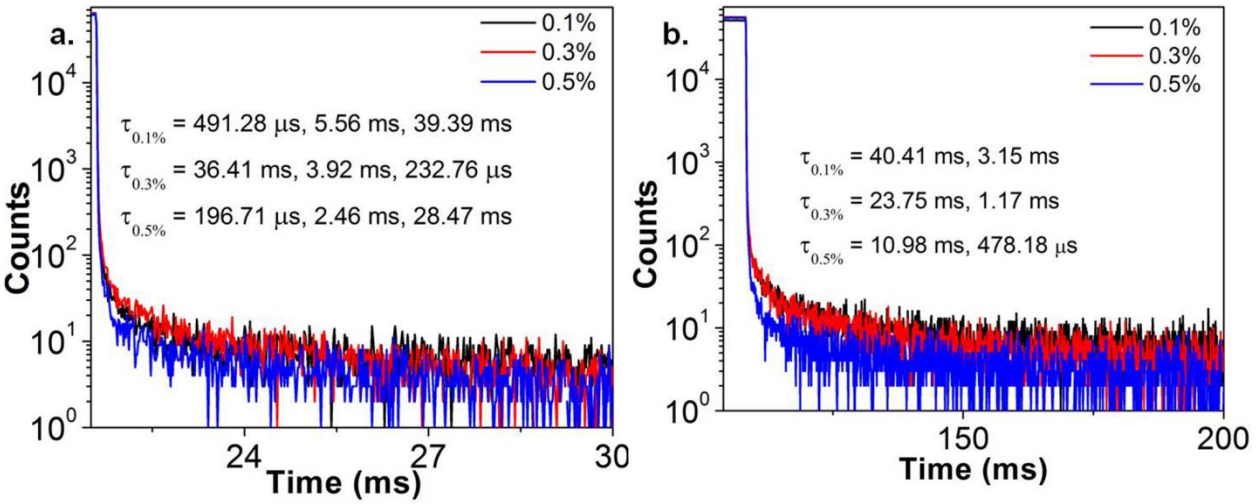

Figure S22. Phosphorescence lifetime measurements of (a) **CPPN** and (b) **CPPNF** at different concentrations in DPEPO (λ_{ex} = 370 nm) at ambient conditions.

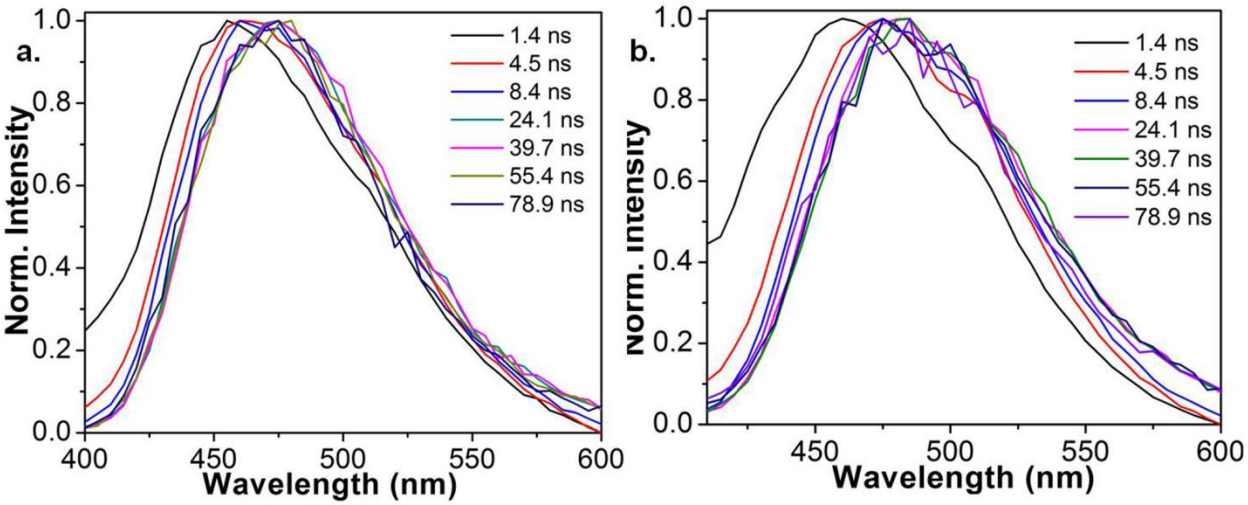

Figure S23. Time resolved fluorescence measurements of (a) **CPPN** and (b) **CPPNF** in 0.1% DPEPO (λ_{ex} = 370 nm) at ambient conditions.

Like PL behaviour observed in PMMA, DPEPO films also show similar emission properties (λ_{ex} = 370 nm) (Figure S24). Emission data collected with the detector delay of 3.4 μs show a blue-shift in the emission spectra of both compounds from 2.98 eV (**CPPN**) and 2.94 eV (**CPPNF**) to 3.00 eV (**CPPN**, **CPPNF**). We confirmed that the species initially formed immediately after 3.4 μs of detector delay is originated due to the delayed fluorescence component populated via the reverse intersystem crossing (rISC) process from $^{3}CT_{CzPN}$. When the DF spectra were compared with the emission peaks observed at 55.4 and 78.4 ns, we found that all the peaks closely overlap with each other thus proves that no new excited state is formed after 55.4 ns. Moreover the overlapping data further proves that $^{1}CT_{CzPN}$ state formed after the slow relaxation as shown in Figure S23 is responsible for TADF.

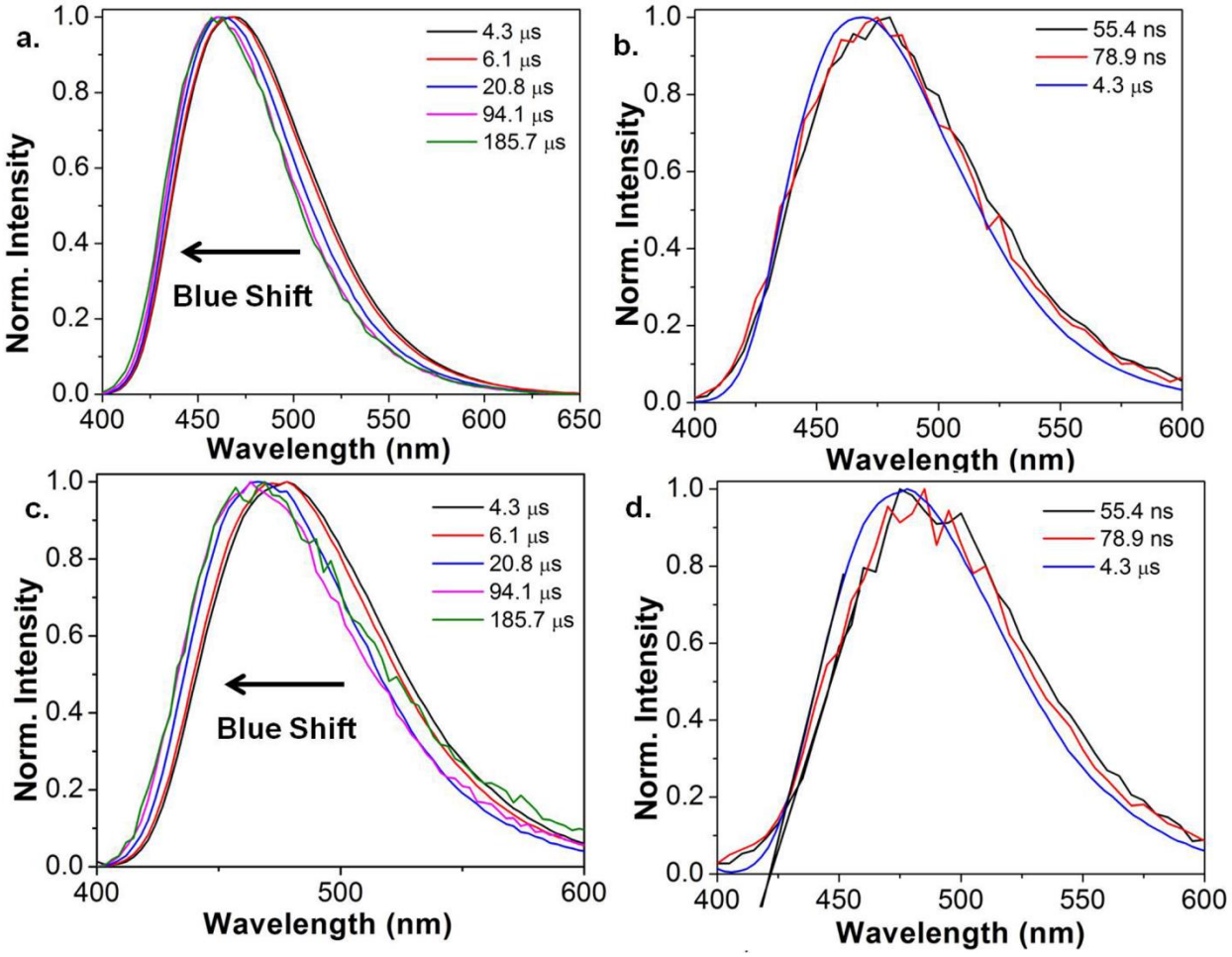

Figure S24. Time resolved emission studies in DPEPO recorded after the detector delay of 3.4 μs (a-b) **CPPN** and (c-d) **CPPNF** (λ_{ex} = 370 nm).

In case of **CPPN** in DPEPO, the energy of the $^3CT_{PPN}$ was calculated from the emission spectra recorded at 185.7 μs with energy at 3.00 eV (Figure S25). The energy of $^1CT_{CzPN}$ was calculated from the emission observed at 4.3 μs with energy at 2.98 eV. The energy of $^3CT_{CzPN}$ was calculated from the emission observed at 55.3 ms after detector delay of 1.75 ms (77 K) with energy at 2.85 eV. In case of **CPPNF** in DPEPO, the energy of the $^3CT_{PPN}$ was calculated from the emission spectra recorded at 185.7 μs (detector delay of 3.4 μs) with energy at 3.00 eV. The energy of $^1CT_{CzPN}$ was calculated from the emission observed at 4.3 μs with energy at 2.94 eV. The energy of $^3CT_{CzPN}$ was calculated from the emission observed at 55.3 ms after detector delay of 1.75 ms (77 K) with energy at 2.85 eV.

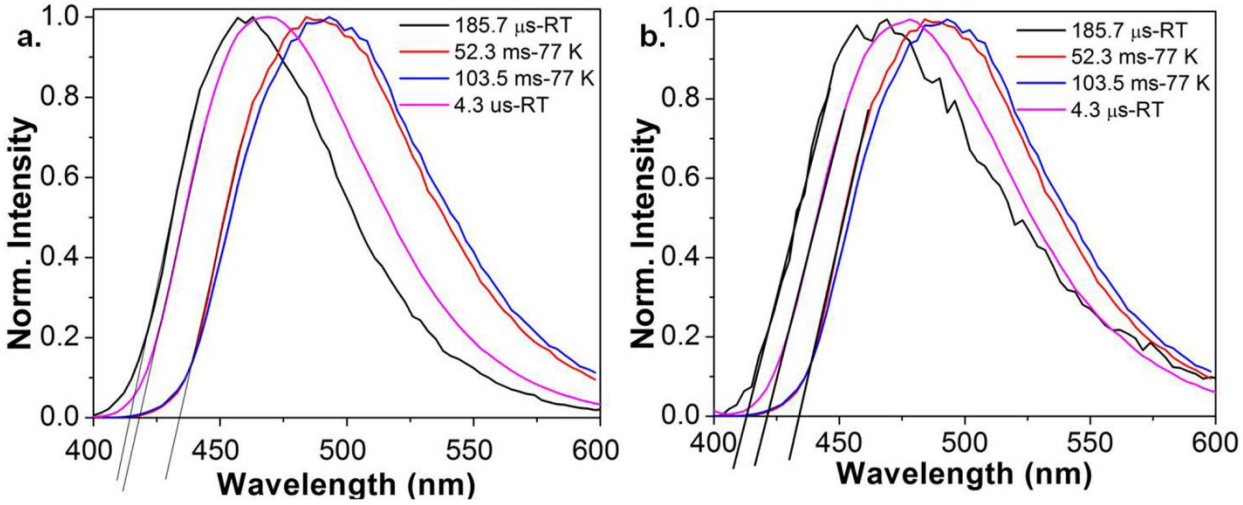

Figure S25. Time resolved emission spectra of (a) **CPPN** and (b) **CPPNF** recorded after 3.4 μs and 1.75 ms of the detector delay (λ_{ex} = 370 nm).

Table S3: Energy levels of the excited states of **CPPN** and **CPPNF** in PMMA and DPEPO.

	PMMA				**DPEPO**			
	$^3LE_{PPN}$ (eV)	**$^1CT_{CzPN}$ (eV)**	**$^3CT_{CzPN}$ (eV)**	**ΔE_{ST} (eV)**	**$^3CT_{PPN}$ (eV)**	**$^1CT_{CzPN}$ (eV)**	**$^3CT_{CzPN}$ (eV)**	**ΔE_{ST} (eV)**
CPPN	3.06	3.01	2.95	0.06	3.00	2.98	2.85	0.13
CPPNF	3.05	3.01	2.94	0.07	3.00	2.94	2.85	0.09

Preparation of PVA films: The stock solution of PVA was made by solubilising 100mg of PVA in 20 ml of deionized water. 1 ml of the stock solution was taken and to it CPPNF solution of THF (1 mg/1 ml) was added keeping the final concentration of the solution to 0.1% w/w PVA-CPPNF. Immediately after adding the THF solution of CPPNF in PVA, turbidity appears due to the formation of the aggregates in the solution. The final solution was further sonicated for 30 minutes. Finally, solution was dropcasted over the quartz plate and kept for drying at 70 ºC for 30 hours to obtain the film.

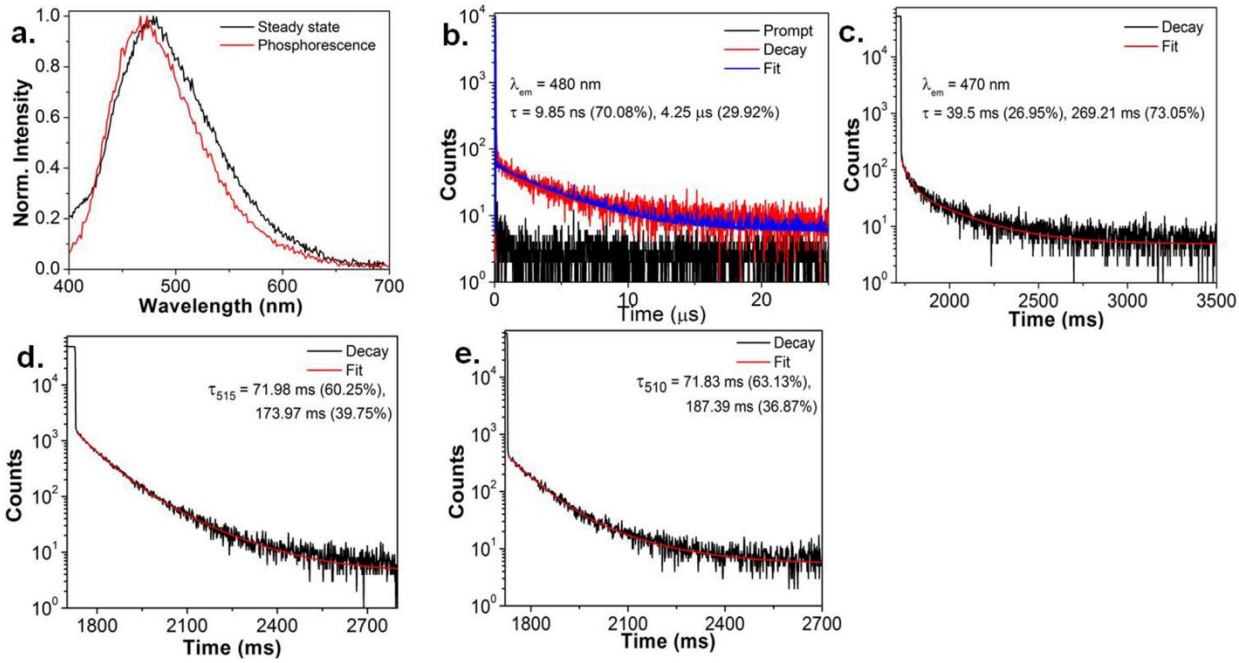

Figure S26. (a) Steady state and phosphorescence (λ_{ex} = 350 nm), (b) Fluorescence lifetime and Phosphorescence lifetime of **CPPNF** in (c) 0.1% PVA films (d) crystals, (e) powder. (λ_{ex} = 370 nm).

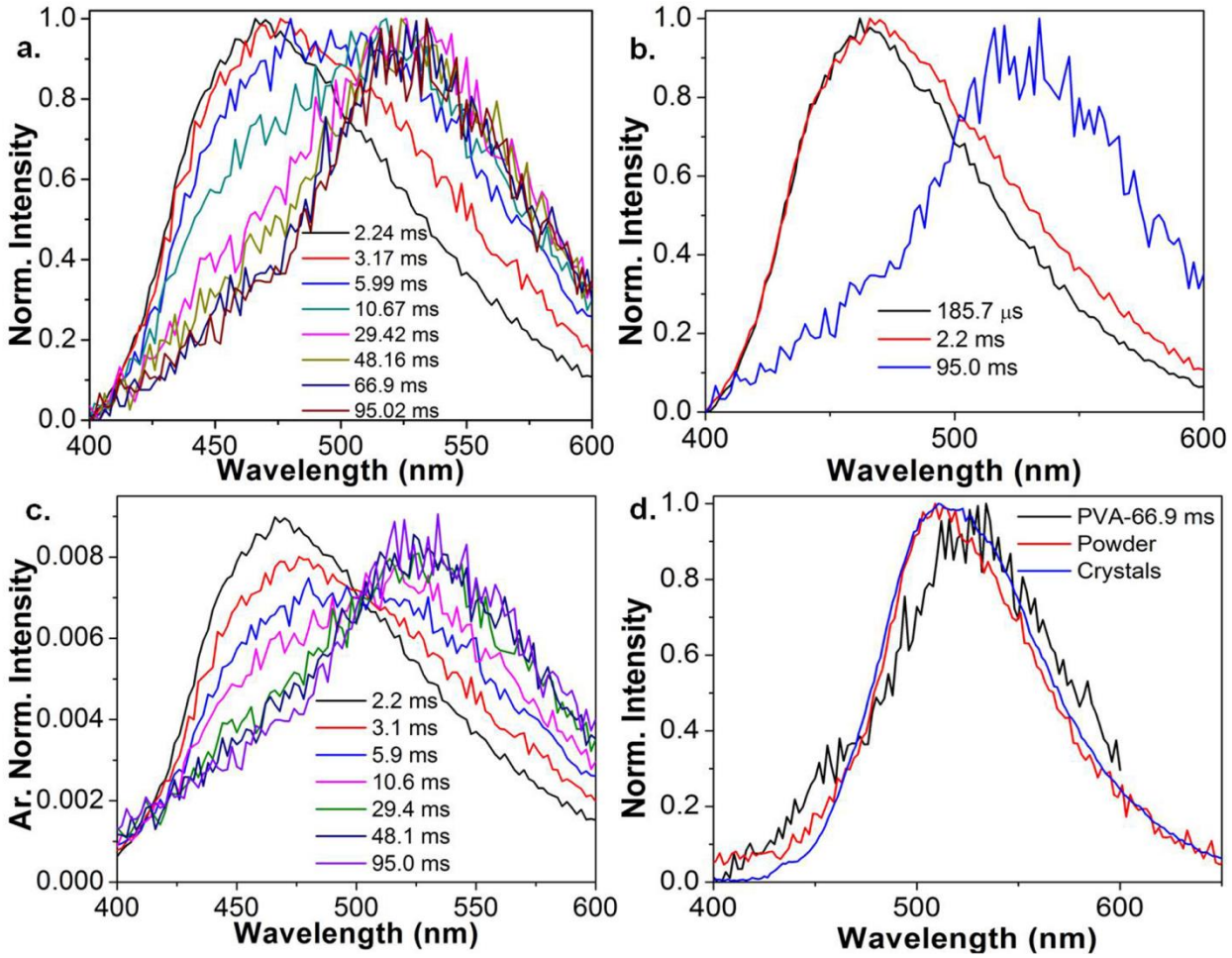

Figure S27. (a) Time resolved emission spectra (TRES) recorded after 1.75 ms of detector delay, (b) Comparison of TRES data and (c) Time resolved area normalized emission spectra (TRANES) of emission recorded after 1.75 ms of the delay for 0.1% CPPNF-PVA films (d) Comparison of the phosphorescence emission spectra recorded in PVA, powder and crystals.

6. Single Crystal Diffraction Analysis

Preparation of CPPN and CPPNF crystals: CPPN/CPPNF (20 mg) was dissolved in HPLC grade 1 mL of dichloromethane and layered with ethanol. The solvent was allowed to evaporate slowly at RT to yield block shaped crystals suitable for X-ray diffraction (95% yield).

X-ray diffraction. Single crystal X-ray diffraction data were collected using a D8 Venture IμS microfocus dual source Bruker APEX3 diffractometer equipped with a PHOTON 100 CMOS detector and an Oxford cryogenic system. Single crystals were mounted at room temperature on the ends of glass fibers and data were collected at room-temperature. Data collection: APEX2 (Bruker, 2014)[2] cell refinement: SAINT (Bruker, 2014)[3] data reduction: SAINT; program(s) used to solve structure: SHELXT (Sheldrick, 2008)[4] program(s) used to refine structure: SHELXL2014 (Sheldrick, 2008); molecular graphics: Ortep-3 for Windows.

Supplementary Table S4: Crystal Parameters

	CPPN	**CPPNF**
CCDC	1990136	1990137
Empirical formula	$C_{44}H_{26}N_4O_2$	$C_{44}H_{22}F_4N_4O_2$
Formula weight	642.69	714.65
Temperature	295(2)	297 (2)
Crystal system	Monoclinic	Monoclinic
Space Group	C 2/c	C 2/c
Unit cell dimensions	a = 22.594(3) Å b = 10.1874(16) Å c = 14.501(3) Å α = 90° β = 98.669(7)° γ = 90°	a = 22.6154(7) Å b = 10.4744(3) Å c = 14.3547(4) Å α = 90° β = 99.9530(10)° γ = 90°
Volume	3299.7(9)	3349.20(17)
Z	4	4
Density(calculated)	1.294	1.417 mg/m^3
Absorption coefficient	0.081 mm^{-1}	0.104 mm^{-1}

F(000)	1336	1464
Crystal size	0.533 × 0.420 × 0.310 mm^3	0.596 × 0.499 × 0.367 mm^3
Theta range for data collection	2.197° to 26.421°	2.50 to 26.01°
Index ranges	-28<= h <=28 -12<=k<=12 -17<= l <=18	-28 <= h <= 27, -13<=k<= 13, -17 <= l <= 17
Reflections collected	20029	28307
Independent reflection	3382	3430
Completeness to θ	99.5%	99.8%
Absorption correction	Multi-scan	Multi-scan
Max. and min. transmission	0.96 and 0.975	0.94 and 0.963
Refinement method	SHELXL-2014/7 (Sheldrick, 2014)	SHELXL-2014/7 (Sheldrick, 2014)
Data / restraints / parameters	3382/0/227	6183 / 0 / 245
Goodness-of-fit on F2	0.960	0.822
Final R indices [I>2σ(I)]	R = 0.0526 wR2 = 0.1187	R = 0.0376 wR2 = 0.0803
R indices(all data)	R = 0.1142 wR2 = 0.1576	R = 0.0615 wR2 = 0.1057
Largest diff. peak and hole	0.172 and -0.154 e.$Å^{-3}$	0.170 and -0.136 e.$Å^{-3}$

References:

1. I. Bhattacharjee, N. Acharya, H. Bhatia, D. Ray, *J. Phys. Chem. Lett.* 2018, **9**, 2733-2738.
2. Bruker APEX2, SAINT and SADABS. Bruker AXS Inc., Madison, Wisconsin, USA, 2014.
3. G. M. Sheldrick, *Acta Cryst. Section* C*: Structural Chemistry*, 2015, **71**, 3-8.
4. L. J. Farrugia, *J. Appl. Cryst.*, 1997, **30**, 565-565.